Fractal spin glass properties of low energy configurations in the Frenkel-Kontorova chain

O. V. Zhirov,[1] G. Casati,[2] and D. L. Shepelyansky[3]
[1]*Budker Institute of Nuclear Physics, 630090 Novosibirsk, Russia*
[2]*International Center for the Study of Dynamical Systems, 22100 Como, Italy*
and Istituto Nazionale di Fisica della Materia and INFN, Unità di Milano, Italy
[3]*Laboratoire de Physique Quantique, UMR C5926 du CNRS, Université Paul Sabatier, 31062 Toulouse, France*
(Received 6 July 2001; published 25 January 2002)

We study, numerically and analytically, the classical one-dimensional Frenkel-Kontorova chain in the regime of pinned phase characterized by phonon gap. Our results show the existence of exponentially many static equilibrium configurations that are exponentially close to the energy of the ground state. The energies of these configurations form a fractal quasidegenerate band structure that is described on the basis of elementary excitations. Contrary to the ground state, the configurations inside these bands are disordered.

DOI: 10.1103/PhysRevE.65.026220 PACS number(s): 05.45.−a, 63.70.+h, 61.44.Fw

The Frenkel-Kontorova (FK) model [1] describes a one-dimensional chain of atoms/particles with harmonic couplings placed in a periodic potential. This model was introduced more than sixty years ago with the aim to study crystal dislocations [1,2]. However, it was also successfully applied for the description of commensurate-incommensurate phase transitions [3], epitaxial monolayers on the crystal surface [4], ionic conductors and glassy materials [5–7] and, more recently, to charge-density waves [8] and dry friction [9–11]. In addition, the FK model has also found its implementation in the investigation of the Josephson junction chain [12]. The physical properties of the FK model are very rich. Moreover, different types of interaction between atoms can be effectively reduced to the case of FK model and, due to that, this model continues to attract the active interest of different research groups.

The ground state of the classical FK model is defined as the static, equilibrium configuration of the chain, which corresponds to the *absolute* minimum of the chain potential energy. More than twenty years ago, Aubry discovered [6,13,14] that the *ground state* is unique and is characterized by a special regular order of atoms in the chain. In fact, the positions of atoms in the chain are described by an area-preserving map, which is well known in the field of dynamical chaos and which is called the Chirikov standard map [15]. The density of particles in the FK model determines the rotation number of the invariant curves of the map, while the amplitude of the periodic potential gives the value of the dimensionless parameter K. For $K<K_c$, the Kolmogorov-Arnold-Moser (KAM) curves are smooth and the spectrum of long wave phonon excitations in the chain is characterized by a linear dispersion law starting from zero frequency. On the contrary for $K>K_c$, the KAM curves are destroyed and replaced by an invariant Cantor set that is called cantorus. In this regime the phonon spectrum has a gap so that the phonon excitations are suppressed at low temperature. The effects of the cantorus on the dynamical properties of the map were discussed in Refs. [16,17]. Later [18], on the example of Ising spin model to which the FK model can be *approximately* reduced [19], it has been shown that the ground state has some well defined hierarchical structure. The main features of this structure are determined by the number properties of the dimensionless particle density that is given by the ratio of the mean interparticle distance to the period of the external field.

In more recent studies [20–23], the attention was mainly concentrated on phonon modes in incommensurate one-dimensional chains. Indeed, the phonon modes contribute to the specific heat of the system and, hence, they are responsible for the heat conduction along the chain [22,23]. The propagation and localization of phonon modes [20,21] have been studied for small vibrations of particles around their equilibrium positions in the *ground state*. In particular, very accurate results were obtained in Ref. [21], where the fractal properties (or self-similarity) of the ground state were used in a very efficient *decimation scheme*.

However, we would like to stress that for $K>K_c$, besides the ground state, there exist other *excited* equilibrium configurations, corresponding to local minima of the potential, with energies very close to the ground state. To our knowledge only few studies were dedicated to excited equilibrium configurations, see, for example Refs. [19,18,24]. In particular, on the example of exactly solvable models, it was found that the number of such configurations can be exponentially large and their energy can be exponentially close to the ground state [25]. In this paper, we study the properties of the low energy equilibrium configurations in the more general case represented by the FK model. We determine the structure of the configuration energy spectrum and its dependence on the strength of the periodic potential and on the chain length. The obtained results show that these configurations are exponentially close in energy to the ground state and the number of configurations grows exponentially with the length of the chain. We also show that these configurations have interesting fractal properties, which we will describe in detail. The transition between different configurations can be understood on the basis of elementary excitations that we call ''bricks.'' The numerical and analytical study of these elementary excitations allows to understand and describe the fractal structure of energy bands corresponding to equilibrium configurations. Since the excited equilibrium configurations are exponentially close to the ground state, they will strongly contribute to the physical system properties at finite temperature. Contrary to the

ground state in which atoms form a regular structure, in the excited configurations this order is partially destroyed and some chaotic feature appears. In some sense, the existence of an exponential number of configurations exponentially close in energy, reminds of the situation in classical spin glasses [26]. However, contrary to the usual spin glass models, the FK model is described by a simple Hamiltonian without any disorder. Therefore, the appearance of exponentially quasidegenerate configurations in the FK system can be viewed as a dynamical spin glass model. Thus, the rich variety of properties of the FK model can find application in different areas of physics.

I. THE MODEL

Let us consider a chain of particles with pairwise elastic interactions between nearest neighbors: $V(x_i,x_{i-1})=v(x_i-x_{i-1})=(x_i-x_{i-1})^2/2$. This chain is placed in a periodic external field: $W(x_i)=-K\cos(x_i)$, where (without any loss of generality) the period is taken equal to 2π. Therefore, the Hamiltonian of the FK model reads

$$H=\sum_i \left[\frac{P_i^2}{2}+\frac{(x_i-x_{i-1})^2}{2}-K\cos(x_i)\right]. \tag{1}$$

Here we have taken the mass of the particles and the elastic constant equal to unity. Thus, all the variables are dimensionless throughout the paper.

At the equilibrium the momenta $P_i=0$ and in addition

$$\frac{\partial H}{\partial x_i}=-x_{i+1}+2x_i-x_{i-1}+K\sin(x_i)=0. \tag{2}$$

After the introduction of new variables $p_{i+1}=x_{i+1}-x_i$, this equation can be written in the form of an area-preserving map

$$p_{i+1}=p_i+K\sin(x_i), \quad x_{i+1}=x_i+p_{i+1}, \tag{3}$$

which is known as the Chirikov standard map [15].

We concentrate our investigation on the case of golden mean dimensionless particle density $\nu=(\sqrt{5}-1)/2$. This irrational value can be approximated by rational approximants that form the Fibonacci sequence s_n with number of particles s and chain length $L=2\pi r$. In this way, the rational approximants are $\nu_n=r_n/s_n=s_{n-1}/s_n$, with $s_n=1,2,3,5,8,13\ldots$ and the average distance between particles is $a=2\pi\nu_n$. For the map (3), the parameter ν determines the rotation number of the invariant KAM curve. At the golden mean value of ν, the KAM curve is analytical and smooth for $K<K_c=0.971\,635\ldots$ [27]. For $K>K_c$, the curve is destroyed and the transition by the breaking of analyticity takes place [6]. As a result, the invariant curve is replaced by a cantorus, which forms an invariant fractal set in the phase space of the map. For the FK model, the cantorus corresponds to the ground state with minimal energy as it was shown by Aubry [6,7,13,14].

In this paper, we restrict ourselves to the case with $K>K_c$, when each particle is locked by potential barriers of the external periodical field and the whole chain is pinned. Stable configurations of the chain correspond to minima of the potential energy:

$$U(\{x\})=\sum_i \left[\frac{(x_i-x_{i-1})^2}{2}-K\cos(x_i)\right]. \tag{4}$$

The static ground state corresponds to *absolute* minimum given by Aubry's solution. However, as we will see in the next section, there are other local minima of the chain potential $U(\{x\})$ that give equilibrium static configurations with energy being very close to the ground state. The number of such configurational states N_{cs} grows exponentially with the chain length s.

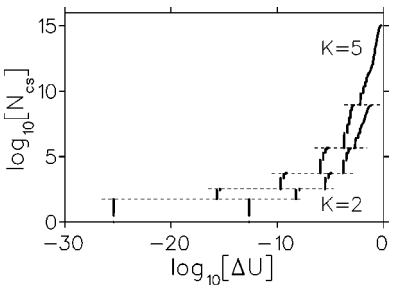

FIG. 1. Integrated number of equilibrium configuration states N_{cs} as a function of the energy difference ΔU between the energy of configuration U and the ground state energy U_G, counted per particle. Here the number of particles is $s=89$ and the number of wells $r=55$. The bands are shown for $K=5$ (6 upper segments) and for $K=2$ (5 lower segments). Horizontal dashed lines show the border between energy bands. All equilibrium configurations are counted. Dimensionless units are used here and in all other figures.

II. ENERGY SPECTRUM OF EQUILIBRIUM CONFIGURATIONS

In Fig. 1, we present a typical result for the integrated number N_{cs} of excited equilibrium configurations versus their energy difference, per particle, from the ground state $\Delta U=(U-U_G)/s$ where U_G is the energy of the ground state. Here we have number of particles $s=89$, number of wells $r=55$ and two values of K, $K=5$ and $K=2$. This figure shows that the energy of configurations form a sequence of narrow energy bands, the width of which is much smaller than the distance between bands, at least in the very vicinity of the ground state. At higher energies, the bandwidth starts to grow and eventually nearest bands almost merge into each other. It is interesting to note that the number of states in each band is practically independent of K, as it is shown by dashed lines in Fig. 1: with the increase of K, each band is shifted to smaller values of ΔU (in logarithmic scale) but the number of states in each band is not changed.

It should be stressed, that even at a moderate value of $K=2$ the energy spacing between the ground state and the first excited configuration band is of the order of 10^{-13}. If one assumes that in Eq. (4) a unit of energy is ~ 1 eV, then this band is already excited at temperature $T\sim 10^{-9}$ K. Hence, one may conclude that the pure ground state is practically

inaccessible, even for a chain with less than one hundred atoms.

The total number of different local minima N_{cs} is enormous and it grows very rapidly with K. Therefore, to numerically find all these configurations, one needs to use special methods. Our approach to this problem is the following. First, we find the ground state by the gradient method developed by Aubry [7,28,29]. Then we find the excited equilibrium configurations with the help of the Metropolis algorithm [30]. In this method, the system is considered at some properly chosen temperature T. At given T, we can probe the configurations with $\Delta U \leqslant T$ while the probability to find configurations with higher energy is exponentially suppressed. Our implementation of the Metropolis algorithm looks as follows. We start from a certain configuration $\{x\}_j$, which corresponds to some local minimum U_j of the chain potential energy $U(\{x\}_j)$. Then, we take randomly one of the chain particles and try to move it into one of the neighboring wells. Next, with the new distribution of particles among the *wells*, we search for a new local minimum $\tilde{U}$. A new configuration with $U_{j+1}=\tilde{U}$ is accepted if $\exp[-(\tilde{U}-U_j)/T] \geqslant \xi$, where ξ is a random number homogeneously distributed in the interval $[0,1]$, otherwise we try a new attempt. Notice that our Metropolis procedure uses particles *jumps* from well to well rather than (small) variations of their coordinates. In this way, we solve the problem of the Peierls-Nabarro barriers [6] and obtain a method with good performance. Physically the Peierls-Nabarro barriers are not important since we are interested in static configurations and not in the transition rate between different states.

In general, the space of low-energy configurations can be viewed as a set of disconnected islands. Therefore, there is a danger that, starting near one island, we can remain in its vicinity forever. To avoid this, we periodically heat/freeze the system. During this process, we perform the above described iterations with chosen temperature T. In this way, the system can move from one island to another and visit different equilibrium configurations.

Since the number of equilibrium configurations is exponentially large (see Fig. 1), it is not possible to visit and count exactly all of them. However, their number can be counted approximately with sufficiently good accuracy in the following way. In the lowest excited band, the number of equilibrium configurations is not so large and it can be computed exactly. In order to determine the number of states in the next band, we start from a representative sample of configurations, which is in fact a small part of their total number in one band. Then with the help of Metropolis algorithm described above, we determine the ratio between the number of configurations inside the first and second band. To do this, we choose the temperature value T in such a way that $T \sim 10\Delta U_2 > \Delta U_1$, where $\Delta U_{1,2}$ are the excitation energies for the first and second band counted from the ground state. From the computed ratio, we determine, with sufficiently good accuracy, the total number of configurations in the second band. By iterating this process, we determine the total number of states in all bands. Moreover, by gradually changing the temperature T, this procedure can be easily adapted to higher excitation energies when the bands begin to merge. This allows to compute the total number of equilibrium configurations in the system, which, for $K=5$ is of the order of 10^{15}.

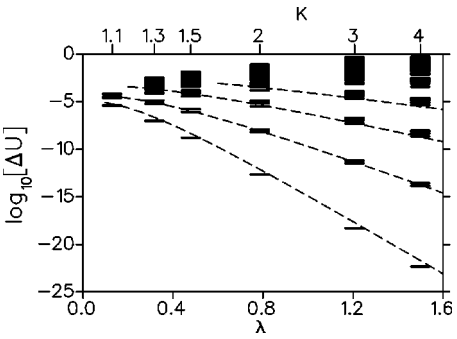

FIG. 2. Band energy spectrum of equilibrium configurations versus the chaos parameter K (upper scale) and the phonon gap λ (lower scale). The bands are marked by filled areas corresponding to a given K value. The chain is the same, as in Fig. 1: $r/s = 55/89$. The dashed curves are given by the semiempirical expression (5).

The energy band spectrum for different values of K is shown in Fig. 2. It clearly shows that the number of bands becomes larger for larger K and, in addition, the lowest bands approach exponentially the ground state. The existence of such bands exponentially close to the ground state is related to the specific properties of the FK chain in the pinned phase ($K > K_c$). This phase is characterized by a phonon gap λ [6,28], due to which any static displacement perturbation δx_{i_0} of particle i_0 (corresponding to a zero-frequency "phonon") decays exponentially along the chain: $\delta x_i \propto \exp(-\lambda \cdot |i-i_0|)$. In fact, λ is the Lyapunov exponent of the map (3) computed on the cantorus. This exponential decay of perturbations is responsible for the appearance of exponentially narrow bands exponentially close to the ground state.

In order to describe the band positions as a function of system parameters, it is convenient to label the bands by the index k in order of increasing energy. Then the energies of the four lowest bands are well described by a simple empirical formula, see Fig. 2,

$$\langle \Delta U_k \rangle \simeq C \exp(-\alpha \nu^k s \sqrt{\beta k + \lambda^2}), \tag{5}$$

where $\langle \Delta U_k \rangle_k$ is the average energy of kth (excited) band, s is the number of particles in the chain, and the numerical values of parameters are $C \approx 1$, $\alpha \approx 0.59$, $\beta \approx 0.12$. It is rather interesting to note that this simple formula describes quite well even the region with small values of $\lambda \leqslant 0.8$ ($K \leqslant 2$). At larger K (and longer chains), this formula can be replaced by its even more simple limiting expression

$$\langle \Delta U_k \rangle \simeq C \exp(-\alpha \nu^k s \lambda). \tag{6}$$

According to Eqs. (5) and (6), the spacings between the bands and the ground state drops exponentially with the length of the chain. In Fig. 3, we present the dependence of

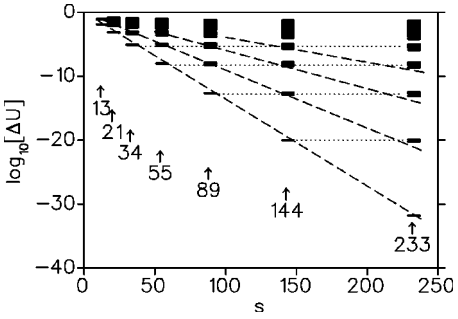

FIG. 3. Dependence of the band energies on the size s of the chain for $K=2$ ($\lambda=0.7859$). Dashed lines are given by empirical formula (5). Horizontal dotted lines allow to compare the band positions for different s.

the band structure on the number of particles s in the chain, for the rational approximants r/s of the golden mean ν.

The results presented in Figs. 2 and 3 show that the simple Semiempirical formula (5), shown by dashed lines, describes the positions of the bands in the interval of 30 orders of magnitude. It is interesting to note that bands are also ordered in some horizontal levels (marked by dotted lines), which are practically independent of the size of the chain. However, the bandwidth and the number of states inside the band of the same horizontal level grows with the chain size s. In the following section, we will see how all these features can be understood on the basis of the spatial properties of the chain structure.

Finally, in Fig. 4 we show that the energy band structure is characterized by fractal properties. Here the third excited band for the chain with $r/s=55/89$ and $K=4$ is shown with subsequently growing resolution (see magnification factors in the figure caption). The hierarchical structure of the bands is evident. Such a structure becomes deeper and deeper with the increase of the chain length s. In the following section, we show the origin of this structure and develop a simple model to describe it.

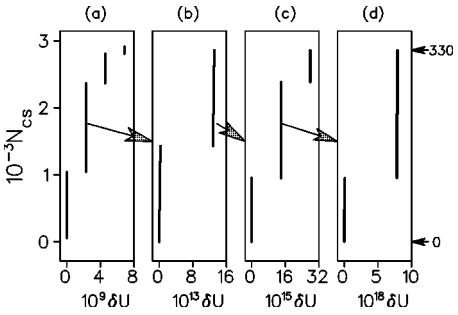

FIG. 4. Fractal energy band structure for a chain with $K=4$, $s=89$, and $r=55$. Four hierarchical levels (a), (b), (c), (d) with growing resolution are shown from left to right. The total magnification factor for δU scale is: 5000 from level (a) to level (b), 2.5×10^5 from (a) to (c), and 8×10^8 from (a) to (d). Here, $\delta U=U-U_{min}$, where U is the chain energy per particle and U_{min} gives the energy of the leftmost band in each panel. The vertical scale N_{cs} gives the integrated number of equilibrium configurations counted from the bottom of the leftmost band in each panel. The vertical magnification is changed in ten times from left to right.

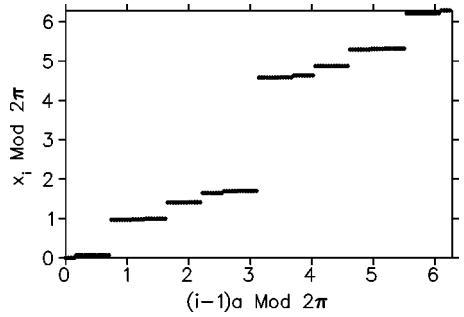

FIG. 5. The particle position x_i mod 2π versus the particle index (multiplied the average distance $a=2\pi r/s$) mod 2π. This hull function is shown for $r=89$, $s=144$, and $K=2$.

III. SPATIAL STRUCTURE OF EQUILIBRIUM CONFIGURATIONS

A. Structure of the ground state

To analyze the origin of the FK chain hierarchical structure, let us start with the study of its *ground state*. It is very instructive to analyze regularities of particle positions inside the wells. In particular, their positions modulo the period of the external field are given by the broadly discussed hull function [7,13,14,28]. Its typical example is presented in Fig. 5.

In this plot, the bottoms of potential wells correspond to x_i mod $2\pi=0$ and 2π. It is easy to see that a considerable amount of particles is located very close to the bottoms. To render this observation even more significant, the absolute values of deviations from the bottom versus the particle number i are plotted in logarithmic scale in Fig. 6.

We see that some of particles are at the well bottoms with extremely good accuracy. Moreover, the values of small deviations are grouped into three well resolved hierarchical levels. Separations along the chain for these particles are also ordered in some regular way. The two particles closest to the bottom $|\Delta x|\approx4.7\times10^{-25}$ are separated by the distances 55 and 89 (the chain is periodic). Then, eight particles (including the previous two) whose deviation from the bottoms is $|\Delta x|\leqslant3\times10^{-6}$, are separated by distances 13 and 21, see Fig. 6. Finally, 34 particles whose deviation from bottoms is $|\Delta x|\leqslant10^{-1}$ are separated by distances 3 and 5. The greater is K, the closer these particles are to the bottoms, yet their separations along the chain remain the same. By taking a

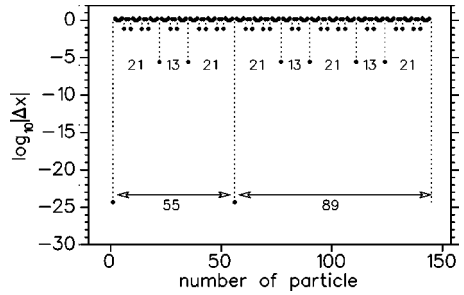

FIG. 6. Absolute value of the particle deviations from the nearest potential well bottom versus particle number along the chain. The chain parameters are as in Fig. 5.

chain with longer length ($r/s=144/233,233/377,377/610,\ldots$) one can observe subsequent levels of the hierarchical structure.

The fact that some particles are very close to the bottom of the wells, is very important. Indeed, let us assume for a moment that these particles are *exactly* at the well bottoms. This means that tension forces acting from both sides on any such particle, called hereafter a ''glue'' particle, balance each other exactly. Now, let us cut the chain at glue particles into fragments, or ''bricks.'' Then we can interchange any two fragments of the chain without changing the chain potential energy. In general, the interchanged bricks are different, and we get in this way a new configuration with the same potential energy. So we may conclude that we can get a combinatorially large number of degenerate configurations in the ground state whose number grows exponentially with the length of the chain.

In fact, our glue particles are lying very close to, but *not exactly* at, the bottoms of wells. Actually, they are slightly shifted from the bottoms, and, therefore, the tensions f at the ends of different bricks are *not* the same. As a consequence, when we exchange two different bricks, each brick's end will be slightly distorted. The distortion is proportional to the difference in boundary tensions Δf of the nearby bricks. This leads to a local change of the chain energy

$$\Delta U \sim \Delta U_b + \Delta U_g , \tag{7}$$

where $\Delta U_b \sim (\Delta f)^2/2$ is due to the distortion of nearby bricks, and $\Delta U_g \approx K(\Delta x)^2/2 = (\Delta f)^2/2K$ is the change of potential energy due to the shift of the glue particle between the bricks. We note that, since glue particle deviations are exponentially small and hierarchically ordered, then the corresponding tension differences are also exponentially small and ordered. Therefore, the energy change caused by bricks permutation depends on the level of the hierarchy inside which the permutation is done. The lowest level of the hierarchy is built by bricks of two types, which consists of two and four particles, respectively. For the sake of brevity, let us denote them as 2 and 4. Then a chain that consists of eight particles can be denoted as $g2g4$ (the letter g stands for a glue particle). The tension difference at this level of the hierarchy is $\Delta f = K\,\Delta x \sim 10^{-1}$.

The next level of hierarchy has bricks $12=(4g2g4)$ and $20=(4g2g4g2g4)$. The brackets are introduced for convenience, to denote the form of the brick. The tension difference at this level is much smaller: $\Delta f = K\,\Delta x \sim 10^{-5}$. Finally, the third level of the hierarchy is composed in the similar way: $54=(20g12g20)$ and $88=(20g12g20g12g20)$, with the corresponding tension difference $\Delta f = K\,\Delta x \sim 10^{-24}$. With increasing particle number, the above described process proceeds in a similar way. A simple estimate for the tension difference valid at any hierarchical level, and for any K, can be written as: $\Delta f \sim K \exp(-\lambda s_{min})$, where s_{min} is the number of particles in the smallest brick at the given level of hierarchy and λ is the phonon gap that depends implicitly on K. Notice that a brick with the addition of the glue particle forms an elementary cell, the size of which is given by the Fibonacci numbers. For example, $(g2)=3,(g4)=5,(g2g4)=8$, etc.

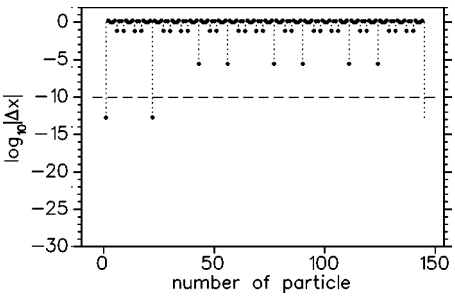

FIG. 7. Deviations of the particles from potential well bottoms for an excited configuration taken from the first excited energy band (see Fig. 3 for $s=144$). The separation of this band from the ground state of Fig. 5 is $\Delta U_1 \sim 10^{-20}$, which implies that the deviations of glue particles from the well bottoms are $\Delta x \leqslant 10^{-10}$ (dashed line).

The composition rules for the brick construction at any hierarchical level can be summarized in following way. Suppose that a given level of hierarchy is composed by two bricks A and B, with the length of A smaller than B. Then the bricks A', B' of the next level can be built as

$$A' = BgAgB, \quad B' = BgAgBgAgBg . \tag{8}$$

Let us note that the hierarchical structure of the ground state has been also considered [18] in the frame of the Ising spin model to which the FK model can be *approximately* reduced [19]. However, we stress that our composition rules differ from those obtained in Ref. [18].

In principle, the composition rules just described allow to build the ground state for a chain of any length. It is also clear that for long enough chains one does not need to search the global minimum of the potential energy. Instead, it is sufficient to minimize the energy of bricks up to some hierarchical level: any further optimization goes beyond any reasonable precision. This, however, also means that within the same precision, the ground state configuration described by Aubry is indistinguishable from exponentially many *disordered* excited configurations.

B. Structure of the excited configurations

The picture of the ground state described above also allows us to understand the structure of excited configurations. However, in this case, the structure can be a bit less self-evident. To illustrate this, in Fig. 7 we plot particles deviations from well bottoms for a configuration from the first excited band in the chain shown in Fig. 6. The hull function for a typical configuration in this band is shown in Fig. 8(a). The hull function for a typical configuration in the second, third, and fourth excited bands (see the band structure in Fig. 3 with $s=144$) is shown in Fig. 8. Contrary to the monotonic hull function of the ground state, here the hull function becomes not monotonic and one can see the overlap between horizontal plateaus.

From Fig. 7, we see that for the first two levels of hierarchy, the deviations of glue particles from the well bottom are

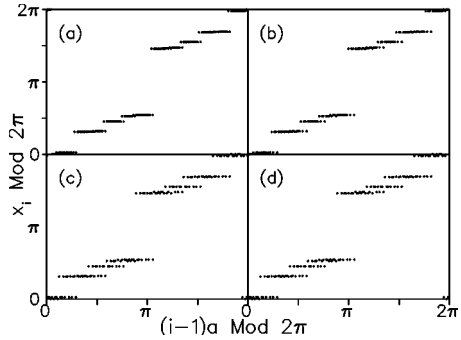

FIG. 8. The hull function for a typical equilibrium configuration in the kth excited band for $K=2$ and $r/s=89/144$: (a) $k=1$, (b) $k=2$, (c) $k=3$, (d) $k=4$. The energy band structure is shown in Fig. 3. Compare with the hull function of the ground state shown in Fig. 5.

practically the same as in the ground state (see Fig. 6). However, at the third hierarchical level the deviations of two glue particles (below the dashed line) become considerably larger than the corresponding ones in the ground state (see Fig. 6).

In order to give an unambiguous definition of bricks, let us remind that we want to split the chain into bricks, whose permutations keep the chain configuration inside the same band. According to Eq. (7), the energy change due to a permutation, produced by the tension differences between permuted bricks, can be estimated as $\delta U\sim(\Delta x)^2$. Therefore, the deviations of glue particles from the bottom between the bricks is restricted by the condition $\Delta x\leqslant(\Delta U_k)^{1/2}$, where ΔU_k is the band energy counted from the ground state. Taking this condition into account, we can write for the configuration shown in Fig. 7 its decomposition into bricks as $g20g122=g20g(20g12g20g12g20g12g20)$, where the expansion of the configuration is shown up to bricks of the second level, 12 and 20. As mentioned above, by brackets we mark the chain fragments in which permutations should be considered as a single brick, since their destruction results in the energy change exceeding the bandwidth.

Let us now discuss the properties of the bricks expansion on the example of a periodical chain with $r/s=89/144$ and $K=2$ (see Fig. 3). The first excited band $k=1$ has the excitation energy $\Delta U_1\approx 9.16\times 10^{-21}$ and is composed from one configuration $g20g(20g12g20g12g20g12g20)$ (here we do not count the configurations with a shift along the chain and reflection). It is interesting to note that this configuration has a long commensurate fragment (123/144).

The second excited band $k=2$ has energy $\Delta U_2\lesssim 10^{-12}$. It is composed by three configurations:

$$g12g20g20g20g12g20g20g12,$$

$$12g20g20g20g20g12g20g12,$$

and

$$g20g20g20g20g20g12g12g12.$$

With the configuration from the first band they give all possible different combinations of three bricks 12 and five bricks 20, which are used in the composition of the ground state.

The third band $k=3$ has the excitation energy $\Delta U_3\lesssim 10^{-8}$. This band has too many configurations to be listed here. Let us, however, mention a new phenomenon that appears in this band, namely, a brick ''chemical'' reaction with dissociation of *larger* elementary bricks of the second hierarchical level,

$$20+20\rightarrow 12+28,\quad 20+28\rightarrow 12+36. \tag{9}$$

Note, that a ''free radical'' 8 coming from dissociation $20\rightarrow 12+8$ is easily captured by other long bricks, so that there is a considerable contribution of long commensurate structures. Near the bottom of the band, a typical configuration is $g20g12g29g12g20g12g12g20$, while at the top, one has $g53g12g12g12g12g12$.

The fourth band $k=4$ has energy $\Delta U_4\lesssim 10^{-5}$. Here we see a dissociation of the bricks from the second hierarchical level,

$$12+20\rightarrow 4+28,\quad 12+28\rightarrow 4+36,\ldots, \tag{10}$$

and appearance of elementary bricks 4 from the first hierarchical level. Here are some examples of configurations in this band with bricks 4:

$$g20g20g28g20g12g12g4g20,$$

$$g12g12g12g28g12g20g4g36,\ldots.$$

Further steps in the whole picture are straightforward. Now we outline a simple theory which turns our qualitative observations into quantitative predictions for the band energy spectrum.

C. An analytical approach

In fact, the construction of bricks is based on the existence of an intrinsic small parameter that allows to develop a simple rapidly converging perturbation theory. Here we outline its main elements. Let us consider the FK chain with s particles and fixed ends at $x_0=0$ and $x_s=2\pi r$. Then the largest brick contains $n=s-1$ particles. If the glue particles $(i=0,i=s)$ are slightly shifted from the well bottoms $x_{a,b}\ll 1$, then the brick energy can be written as

$$U^{(n)}(x_a,x_b)=U_0^{(n)}-f_a^{(n)}x_a+f_b^{(n)}x_b++R_a^{(n)}\frac{x_a^2}{2}+R_b^{(n)}\frac{x_b^2}{2}$$
$$-T^{(n)}x_a x_b, \tag{11}$$

where $U_0^{(n)}=U^{(n)}(0,0)$ is the unperturbed energy, $f_{a,b}^{(n)}$ and $R_{a,b}^{(n)}$ are tensions and rigidities at the left/right ends of the brick, and $T^{(n)}$ is the static ''transmission'' factor along the brick with n particles. If the brick is symmetric then $f_a^{(n)}=f_b^{(n)}\equiv f^{(n)}$ and $R_a^{(n)}=R_b^{(n)}\equiv R^{(n)}$. The key point of the theory is that in the presence of a nonzero phonon gap λ, the transmission factor $T^{(n)}$ is exponentially small: $T^{(n)}$

$\sim \exp(-\lambda n)$. Therefore, it can be very efficiently used as an expansion parameter in the calculations of the energy band spectrum.

Suppose that at some hierarchical level we have two elementary bricks A and B, with lengths $n_A < n_B$. According to our rule of brick composition (8), we can calculate the energy of the brick $A' = BgAgB$ as,

$$U^{(A')}(x_a, x_b) = \min_{x_1 x_2}[U^B(x_a, x_1) + U^A(x_1, x_2) + U^B(x_2, x_b)]. \tag{12}$$

Then, rewriting Eq. (12) in the form (11), we obtain the transformation rules for brick parameters R, f, and T. In the leading order approximation in the small parameter T, these rules have the form

$$R^{A'} = R^A,$$

$$f^{A'} = f^B - \frac{T^B(f^B - f^A)}{R^A + R^B + K} + \cdots, \tag{13}$$

$$T^{A'} = \frac{T^A (T^B)^2}{(R^A + R^B + K)^2}.$$

In the same way for B' we obtain

$$R^{B'} = R^B,$$

$$f^{B'} = f^{A'} + (\Delta f)', \tag{14}$$

$$T^{B'} = \frac{T^B (T^A T^B)^2}{(R^A + R^B + K)^4},$$

where the tension difference $(\Delta f)' = f^{B'} - f^{A'}$ between new bricks A' and B' can be expressed through the brick tension difference $(\Delta f) = f^B - f^A$ as

$$(\Delta f)' = -\frac{T^A (T^B)^2}{(R^A + R^B + K)^2}(\Delta f). \tag{15}$$

To apply these transformation rules, one needs to know the bricks parameters at the lowest hierarchical level, e.g., for bricks 2 and 4. In this case, the number of particles is small and the expansion (11) can be performed analytically. For the case $K=2$ considered above, we get $T^{(2)} = 0.24$, $R^{(2)} = 0.454$, $T^{(4)} = 0.0533$, $R^{(4)} = 0.32$, and $(\Delta f)^{(2,4)} = 0.21$. By applying the transformation rules to these data, we obtain for the bricks of the next hierarchical level 12 and 20: $T^{(12)} = 8.86 \times 10^{-5}$, $T^{(20)} = 1.796 \times 10^{-7}$, $(\Delta f)^{(12,20)} = -6.93 \times 10^{-6}$. The exact numerical simulation gives $T^{(12)} = 9.82 \times 10^{-5}$, $T^{(20)} = 1.799 \times 10^{-7}$, $(\Delta f)^{(12,20)} = -7.16 \times 10^{-6}$. Starting with exact values for bricks 12 and 20, the transformation rules give for bricks 54 and 89, results which are correct within four digits accuracy.

Therefore, this simple approach can quantitatively explain the splitting of the whole spectra into bands. Surely, the leading terms in the small parameter T, as well as the expansion (11), can be insufficient to reproduce with high accuracy, the deep levels of hierarchical band structure. To this end, one should take into account higher order terms.

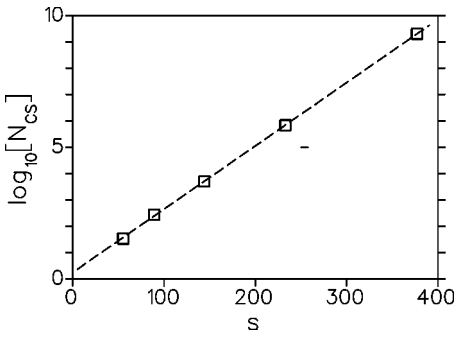

FIG. 9. The number of equilibrium configurations N_{cs} with excitation energy from the ground state $\Delta U \leqslant 2 \times 10^{-8}$ as a function of the number of particles s in the chain for $K=2$. The dashed line shows the fitted exponential dependence $N_{cs} = 1.78 \exp(0.0554 s)$.

The results presented in this section show that the number of equilibrium configurations grows very quickly with the length of the chain and with the chaos parameter K. These configurations form bands that are placed exponentially close to the ground state. As a result, even in a fixed very small vicinity of the ground state, the number of configurations grows exponentially with the chain length. This fact is illustrated in Fig. 9.

IV. DISCUSSION AND CONCLUSIONS

In this paper, we studied the properties of equilibrium static configurations in the Frenkel-Kontorova chain in the regime of pinned phase characterized by phonon gap. This FK model is rather general and finds applications not only for commensurate-incommensurate transition for atoms placed on a periodic substrate but also in many other fields of physics. In addition, near the equilibrium, also the cases with long range interactions between atoms can be effectively reduced to the FK model with only nearest neighbors interaction. We have shown that energies of equilibrium configurations form a hierarchical band structure so that exponentially many configurations become exponentially close to the unique ground state. In this respect, the FK model has certain similarities with classical spin glass models, which also are characterized by existence of exponentially many quasidegenerate states [26]. At the same time, in the FK model the disorder is absent and the quasidegenerate configurations form a fractal sequence of energy bands, which in a sense can be considered a dynamical spin glass. On the basis of extended numerical and analytical investigations, we determined the low energy excitation inside the quasidegenerate bands that have a form of bricks from which the whole chain can be composed. On the basis of these results, we have shown that while the ground state is characterized by regular structure, the low energy excited configurations are disordered due to elementary brick displacements. This means that exponentially close to the ground state, there are disordered configurations that may have rather different physical properties compared to the ground state. For example, this

disorder should significantly affect the properties of phonon excitations in the chain. The exponential quasidegeneracy of low energy configurations should be also important in the case of quantum FK chain when quantum particles can tunnel from one configuration to another. These two aspects are related to new interesting physical effects of low energy excitations in many-body systems and require further investigations [31].

ACKNOWLEDGMENTS

This work was supported in part by the EC RTN network contract HPRN–CT-2000-0156. One of us (O.V.Z.) thanks Cariplo Foundation, INFN, and RFBR Grant No. 01-02-17621 for financial support. Support from the PA INFN ''Quantum Transport and Classical Chaos'' is gratefully acknowledged.

[1] Y. I. Frenkel and T. K. Kotorova, Zh. Eksp. Teor. Fiz. **8**, 1340 (1938) [Phys. Z. Sowjetunion **13**, 1 (1938)].
[2] F. Nabarro, *Theory of Crystal Dislocations* (Clarendon, Oxford, 1967).
[3] V. L. Pokrovsky and A. L. Talapov, *Theory of Incommensurate Crystals* (Harwood, London, 1984), Vol. 1.
[4] S. C. Ying, Phys. Rev. B **3**, 4160 (1971).
[5] L. Pietronero, W. R. Schneider, and S. Sträsler, Phys. Rev. B **24**, 2187 (1981).
[6] S. Aubry, in *Solitons and Condensed Matter Physics*, edited by A. R. Bishop and T. Schneider (Springer, New York, 1978).
[7] S. Aubry, J. Phys. (France) **44**, 147 (1983).
[8] L. M. Floria and J. J. Mazo, Adv. Phys. **45**, 505 (1996).
[9] O. M. Braun, T. Dauxois, M. V. Paliy, and M. Peyrard, Phys. Rev. Lett. **78**, 1295 (1997); Phys. Rev. E **55**, 3598 (1997).
[10] M. Weiss and F. J. Elmer, Phys. Rev. B **53**, 7539 (1996); Z. Phys. B: Condens. Matter **104**, 55 (1997).
[11] L. Consoli, H. J. F. Knops, and A. Fasolino, Phys. Rev. Lett. **85**, 302 (2000).
[12] S. Watanabe, H. S. J. van der Zant, S. N. Strogatz, and T. P. Orlando, Physica D **97**, 429 (1996).
[13] S. Aubry, Physica D **7**, 240 (1983).
[14] S. Aubry and P. Y. Le Daeron, Physica D **8**, 381 (1983).
[15] B. V. Chirkov, Phys. Rep. **52**, 263 (1979).
[16] I. C. Percival, *Nonlinear Dynamics and the Beam-Beam Interaction*, edited by Melvin Month and John Herrera, AIP Conf. Proc. No. 57 (AIP, New York, 1979), p. 302.
[17] R. S. MacKay, J. D. Meiss, and I. C. Percival, Physica D **13**, 55 (1984).
[18] F. Vallet, R. Schilling, and S. Aubry, Europhys. Lett. **2**, 815 (1986); J. Phys. C **21**, 67 (1988).
[19] H. U. Beyeler, L. Pietronero, and S. Strässler, Phys. Rev. B **22**, 2988 (1980).
[20] E. Burkov, B. E. C. Koltenbah, and L. W. Bruch, Phys. Rev. B **53**, 14 179 (1996).
[21] J. A. Ketoja and I. I. Satija, Physica D **104**, 239 (1997); e-print cond-mat/9802149.
[22] P. Tong, B. Li, and B. Hu, Phys. Rev. B **59**, 8639 (1999).
[23] B. Hu, B. Li, and H. Zhao, Phys. Rev. E **61**, 3828 (2000).
[24] S. Aubry and G. Abramovici, Physica D **43**, 199 (1990).
[25] R. Schilling, Phys. Rev. Lett. **53**, 2258 (1984); P. Reichert and R. Schilling, Phys. Rev. B **32**, 5731 (1985).
[26] M. Mézard, G. Parisi, and M. A. Virasoro, *Spin Glass Theory and Beyond* (World Scientific, Singapore, 1997).
[27] J. M. Greene, J. Math. Phys. **20**, 6 (1979); R. S. MacKay, Physica D **7**, 283 (1983).
[28] M. Peyrard and S. Aubry, J. Phys. C **16**, 1593 (1983).
[29] H. J. Schellnhuber, H. Urbschat, and A. Block, Phys. Rev. A **33**, 2856 (1986).
[30] M. Creutz and B. Freedman, Ann. Phys. (N.Y.) **132**, 427 (1981).
[31] O. V. Zhirov, G. Casati, and D. L. Shepelyansky (unpublished).